

# Supplementary Materials

Anonymous Authors

## 1 REVIEW OF SPHERICAL HARMONICS

This part is mainly cited from [3].

**Definition** Spherical harmonics define an orthonormal (to get the proof of this, please refer to [2]) basis over the sphere,  $\mathbf{S}$ , analogous to the Fourier transform over the 1D circle. Using the parameterization:

$$s = (x, y, z) = (\sin\theta\cos\phi, \sin\theta\sin\phi, \cos\theta) \quad (1)$$

the basis functions are defined as

$$Y_l^m(\theta, \phi) = K_l^m e^{im\phi} P_l^{|m|}, l \in \mathbb{N}, m \in (-l, l) \quad (2)$$

where  $P_l^{|m|}$  are the associated Legendre polynomials and  $K_l^m$  are the normalization constants

$$K_l^m = \sqrt{\frac{(2l+1)(l-|m|)!}{4\pi(l+|m|)!}} \quad (3)$$

The above definition forms a complex basis; a real-valued basis is given by the simple transformation:

$$y_l^m = \begin{cases} \sqrt{2}K_l^m \cos(m\phi) P_l^m \cos\theta & m > 0 \\ \sqrt{2}K_l^m \sin(-m\phi) P_l^m \cos\theta & m < 0 \\ \sqrt{2}K_0^0 P_0^0 \cos\theta & m = 0 \end{cases} \quad (4)$$

Low values of  $l$  (called the band index) represent low-frequency basis functions over the sphere. The basis functions for band  $l$  reduce to polynomials of order  $l$  in  $x$ ,  $y$ , and  $z$ . **Projection and**

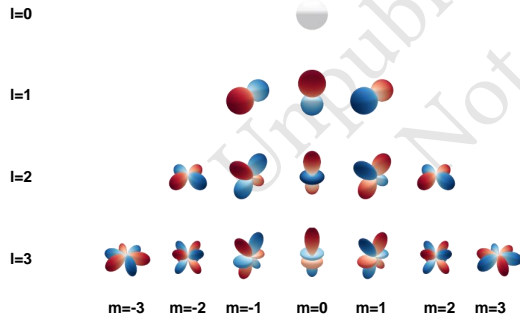


Figure 1: Spherical Harmonics

**Reconstruction** Any function  $F(s)$  defined on the sphere  $S$  can be represented as a set of SH basis functions:

$$F(s) \approx \sum_{l=0}^{n-1} \sum_{m=-l}^l f_l^m Y_l^m(s) = \tilde{F}(s) \quad (5)$$

where  $n$  denotes the degree of SH and  $Y_l^m(s)$  is a set of real basis of SH.  $\tilde{F}(s)$  is the  $n$ -th order reconstruction function which approximates  $f$  increasingly well as the number of bands  $n$  increases.

2024-04-19 06:20. Page 1 of 1-4.

Because the SH basis is orthonormal, the scalar function  $F$  can be projected into its coefficients via the integral:

$$f_l^m = \int F(s) Y_l^m(s) ds \quad (6)$$

Low-frequency signals can be accurately represented with only a few SH bands. It is often convenient to rewrite 7 in terms of a singly indexed vector of projection coefficients and basis functions, via:

$$F(s) \approx \sum_{i=0}^{n^2-1} f_i Y_i(s) = \tilde{F}(s) \quad (7)$$

where  $i = l(l+1) + m + 1$ .

**Basic Properties** A critical property of SH projection is its rotational invariance; that is, given:  $g(s) = F(Q(s))$  where  $Q$  is an arbitrary rotation over  $S$  then:

$$\tilde{g}(s) = \tilde{F}(Q(s)) \quad (8)$$

Orthonormality of the SH basis provides the useful property that given any two functions  $a$  and  $b$  over  $S$ , their projections satisfy:

$$\int a(s)b(s)ds = \sum_{i=0}^{n^2-1} a_i b_i \quad (9)$$

since

$$\int_{\Omega} Y_p(s) Y_q(s) ds = \begin{cases} 1 & \text{if } p = q \\ 0 & \text{otherwise} \end{cases} \quad (10)$$

**Product Projection** Projection of the product of a pair of spherical functions  $c(s) = a(s)b(s)$  where  $a$  is known and  $b$  unknown can be viewed as a linear transformation of the projection coefficients  $b_j$  via a matrix :

$$c(s) = \int a(s)(b_j y_j(s)) y_i(s) ds \quad (11)$$

$$= b_j a_k \int y_j(s) y_i(s) y_k(s) = \tilde{a}_{ij} b_j \quad (12)$$

where summation is implied over the duplicated  $j$  and  $k$  indices. Note that  $\tilde{a}$  is a symmetric matrix.

## 2 DETAILS OF GRADIENT COMPUTATION

In section 4, we claim that our pipeline is differentiable, we will provide the detail proof of and show the gradient computation. From section 4.5 we have:

$$T(\omega_o, \omega_i) = \sum_{i=1}^{m^2} \sum_{j=1}^{n^2} t'_{ij} Y_j(\omega_o) Y_i(\omega_i) \quad (13)$$

where:

$$t'_{ij} = \sum_{l=1}^q \sum_{k=1}^p Y^i(\omega_l^l) T(\omega_l^l, \omega_o^l) Y^j(\omega_o^k) \quad (14)$$



Figure 2: High-quality relighting results achieved by our proposed method on TensorIR dataset

and

$$L_o(x) = \sum_{i=0}^{m^2} \sum_{j=0}^{n^2} l_i t'_{ij} = \tilde{L} \cdot T_{n \times n}^{final} \quad (15)$$

Further, we have:

$$T^{final} = Y_{n \times m}^i T_{m \times m} Y_{m \times n}^j \quad (16)$$

if we use the same sampler for  $Y^i$  and  $Y^j$  we have:

$$Y^i = \text{transpose}(Y^j) \quad (17)$$

Finally, we have:

$$T^{final} = YTY^T \quad (18)$$

where:

$$Y = \begin{pmatrix} y_{11} & y_{12} & \dots & y_{1m} \\ y_{21} & y_{22} & \dots & y_{2m} \\ \vdots & \vdots & \ddots & \vdots \\ y_{n1} & y_{n2} & \dots & y_{nm} \end{pmatrix} \quad (19)$$

and:

$$y_{ij} = Y_i(\omega_j) \quad (20)$$

represent the spherical harmonics basis function result at the direction  $\omega_j$ . We also have:

$$T = \begin{pmatrix} t_{11} & t_{12} & \dots & t_{1m} \\ t_{21} & t_{22} & \dots & t_{2m} \\ \vdots & \vdots & \ddots & \vdots \\ t_{m1} & t_{m2} & \dots & t_{mm} \end{pmatrix} \quad (21)$$

where:

$$t_{ij} = (1 - m) \frac{\rho}{\pi} + \frac{DFG}{4(\omega_i \cdot n)(\omega_j \cdot n)} (\omega_i \cdot n) V(\omega_i, x) d\omega_i \quad (22)$$

We can apply the chain rule to find the derivatives w.r.t.  $\rho$ ,  $D$ ,  $F, G$  and get the derivatives of  $m$  and  $r$  by  $D, F, G$ . To simplify the representation, we use  $\rho$  as an example:

$$\frac{\partial T^{final}}{\partial \rho} = \frac{\partial T^{final}}{\partial T} \frac{\partial T}{\partial \rho} \quad (23)$$

where:

$$\frac{\partial T^{final}}{\partial T} = YY^T \quad (24)$$

and

$$\frac{\partial t_{ij}}{\partial \rho} = \frac{(1 - m)}{\pi} \quad (25)$$



Figure 3: High-quality relighting results achieved by our proposed method on DTU dataset [1].

we have:

$$\frac{\partial \mathbf{T}^{\text{final}}}{\partial \rho} = \begin{pmatrix} t'_{11} & t'_{12} & \cdots & t'_{1m} \\ t'_{21} & t'_{22} & \cdots & t'_{2m} \\ \vdots & \vdots & \ddots & \vdots \\ t'_{m1} & t'_{m2} & \cdots & t'_{mm} \end{pmatrix} \quad (26)$$

and:

$$t'_{ij} = \frac{(1-m)}{\pi} Y_i(\omega_j) Y_j(\omega_i) \quad (27)$$

### 3 RESULTS ON TENSOIR SYNTHETIC DATASET

Tab 1 provides the results on normal estimation, novel view synthesis, and relighting for all scenes. We also visualize the relighting results of PRTGS in Fig 2.

### 4 RESULTS ON REAL-WORLD DATASET

For the real-world Dataset, we list the results on novel view synthesis (i.e.PSNR, SSIM, and LPIPS) of PRTGS and some NeRF variants in Tabs 2, 3 and 4. In addition, we provide the relighting results of all seven publicly available scenes in Fig 3.

**Table 1: TensolR dataset**

Scene	Method	Novel View Synthesis			Relight		
		PSNR $\uparrow$	SSIM $\uparrow$	LPIPS $\downarrow$	PSNR $\uparrow$	SSIM $\uparrow$	LPIPS $\downarrow$
Lego	NeRFactor	26.076	0.881	0.151	23.246	0.865	0.156
	InvRender	24.391	0.883	0.151	20.117	0.832	0.171
	NVDiffrec	30.056	0.945	0.059	20.088	0.844	0.114
	TensolR	34.700	0.968	0.037	28.581	0.944	0.081
	Gsir	34.379	0.968	0.036	23.256	0.842	0.117
	Relightable	36.741	0.976	0.024	21.860	0.834	0.115
	Ours	37.830	0.980	0.020	24.005	0.879	0.095
Armadillo	NeRFactor	26.479	0.947	0.095	26.887	0.944	0.102
	InvRender	31.116	0.968	0.057	27.814	0.949	0.069
	NVDiffrec	33.664	0.983	0.031	23.099	0.921	0.063
	TensolR	39.050	0.986	0.039	34.504	0.975	0.045
	Gsir	39.287	0.980	0.039	27.737	0.918	0.091
	Ours	46.917	0.991	0.024	32.443	0.947	0.050
Ficus	NeRFactor	21.664	0.919	0.095	20.684	0.907	0.107
	InvRender	22.131	0.934	0.057	20.330	0.895	0.073
	NVDiffrec	22.131	0.946	0.064	17.260	0.865	0.073
	TensolR	29.780	0.973	0.041	24.296	0.947	0.068
	Gsir	33.551	0.976	0.031	24.932	0.893	0.081
	Relightable	37.830	0.989	0.013	26.584	0.896	0.081
	Ours	41.207	0.994	0.012	26.721	0.888	0.076

**Table 2: MipNerf360 psnr**

Method	bicycle	garden	stump	room	counter	kitchen	bonsai
NeRF++	22.64	24.32	24.34	28.87	26.38	27.80	29.15
Plenoxels	21.91	23.49	20.66	27.59	23.62	23.42	24.67
INGP-Base	22.19	24.60	23.63	29.27	26.44	28.55	30.34
INGP-Big	22.17	25.07	23.47	29.69	26.69	29.48	30.69
Gsir	23.68	25.47	25.22	29.56	26.16	27.90	28.65
Ours	25.919	31.223	30.563	24.479	26.864	27.82	29.946

**Table 3: MipNerf360 ssim**

Method	bicycle	garden	stump	room	counter	kitchen	bonsai
NeRF++	0.455	0.546	0.453	0.843	0.775	0.749	0.792
Plenoxels	0.496	0.606	0.523	0.842	0.759	0.648	0.814
INGP-Base	0.491	0.649	0.574	0.855	0.798	0.818	0.890
INGP-Big	0.512	0.701	0.594	0.871	0.817	0.858	0.906
Gsir	0.686	0.791	0.707	0.888	0.850	0.874	0.909
Ours	0.763	0.934	0.942	0.744	0.843	0.907	0.921

**Table 4: MipNerf360 lpips**

Method	bicycle	garden	stump	room	counter	kitchen	bonsai
NeRF++	0.455	0.331	0.416	0.335	0.351	0.260	0.291
Plenoxels	0.506	0.386	0.503	0.419	0.441	0.447	0.398
INGP-Base	0.487	0.312	0.450	0.301	0.342	0.254	0.227
INGP-Big	0.446	0.257	0.421	0.261	0.306	0.195	0.205
Gsir	0.296	0.181	0.294	0.244	0.243	0.118	0.231
Ours	0.248	0.168	0.156	0.246	0.158	0.174	0.126

## REFERENCES

- [1] Rasmus Jensen, Anders Dahl, George Vogiatzis, Engin Tola, and Henrik Aanaes. 2014. Large scale multi-view stereopsis evaluation. In *Proceedings of the IEEE conference on computer vision and pattern recognition*. 406–413.
- [2] Volker Schönefeld. 2005. Spherical harmonics. *Computer Graphics and Multimedia Group, Technical Note. RWTH Aachen University, Germany* 18 (2005).
- [3] Peter-Pike Sloan, Jan Kautz, and John Snyder. 2002. Precomputed Radiance Transfer for Real-Time Rendering in Dynamic, Low-Frequency Lighting Environments. (2002).